FATIGUE AND POST-FATIGUE BEHAVIOUR OF CARBON/EPOXY NON CRIMP FABRIC COMPOSITES

Katleen Vallons*, Stepan V. Lomov*, Ignaas Verpoest*
***Department of Metallurgy and Materials Engineering, Katholieke Universiteit Leuven,**

Keywords: *Non crimp fabric, mechanical properties, fatigue, carbon fibre composites*

Abstract

The properties of a carbon/epoxy biaxial ±45 non crimp fabric composite are studied. The damage initiation stress-strain level in a static test was determined for different test directions. This damage initiation stress level was then taken as the maximum stress level for tensile-tensile fatigue tests in the fibre directions. In the matrix-dominated directions, fatigue tests were done up to the stress level corresponding to the onset of non-linear behaviour in a tensile test. For both fibre- and matrix-dominated directions, samples did not break up to 5x10^6 cycles. No significant stiffness decrease was measured, but samples in the fibre directions showed an increasing density of transverse matrix cracks. To evaluate the influence of the fatigue cycling on the material properties, post-fatigue tensile tests were done. The fatigue life of the material at higher load levels was also investigated.

1 Introduction

Non crimp fabrics (NCFs) combine the good drapeability of woven fabrics with a very low crimp and numerous other advantages, making them an attractive material for use in high-performance composite parts.

Research concerning NCF composites has been conducted in the recent past, and a number of interesting papers have been published. In [1-4], Edgren investigated several properties of NCF composites, including the compression behaviour and the formation of damage in tension. In another series of papers [5-10], a variety of aspects of NCFs is covered: in [5-8], a comprehensive study of the behaviour of several carbon fibre non crimp fabrics can be found, including modelling of the internal geometry of undeformed, compressed and sheared fabrics, characterisation of the behaviour of the dry fabrics in tension, shear, bending, compression and friction.

In part 4 and 6 of the series [9, 10], the mechanical properties of several kinds of carbon fibre NCF composites are investigated, as well as the damage initiation and development during static tensile testing and the characterisation of the fatigue behaviour at low loads.

As it is described in [9], a static tensile test can be divided in three stages, based on the damage development: in the first stage, no detectable damage is formed in the sample. In the second stage, damage starts and grows, and in the last stage, final failure occurs. These three stages can be determined with the use of acoustic emission. The cumulative acoustic emission energy curve shows distinct changes in slope in the transition areas between the different phases. The first of these transitions is called the damage initiation stress/strain level and is denoted ε_a. For one of the NCF composites, the fatigue behaviour at a stress up to the damage initiation stress was investigated [10]. It was found that in fibre direction, fatigue life exceeded 10^6, and transverse cracks were seen to develop during the fatigue cycling. Also, a small decrease in tensile modulus was observed. In bias direction, matrix cracks running parallel to the fibres were seen to develop, and the samples had an average fatigue life of $3x10^5$ cycles. A clear stiffness decrease was observed during the tests.

In this paper, the same methodology will be used to determine the fatigue behaviour of another biaxial carbon fibre – epoxy NCF composite at low loads (corresponding to the damage initiation load in a static test). Also, the fatigue life at higher loads will be investigated.

2 Materials and production

A picture of the ±45 biaxial carbon fibre non crimp fabric used for the study can be seen in figure 1. The areal density of the fabric is 540 g/m². The

internal parameters of the fabric have been characterised and can be found in table 1.

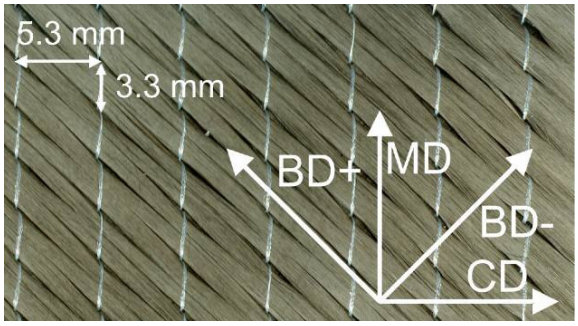

Fig. 1. The ±45 carbon fibre non crimp fabric used in this study, and the four test directions

Table 1: Internal characteristics of the ±45 NCF

	+45/-45 NCF
Opening length (front), mm	9.6 ± 1.6
Opening length (back), mm	11.9 ± 1.3
Opening width (front), mm	0.26 ± 0.01
Opening width (back), mm	0.23 ± 0.03
Spacing stitches, mm	5.3 ± 0.1
Length stitches, mm	3.3 ± 0.4

Composite plates are produced from the fabric, which is prelaminated with a epoxy resin layer. The production consists of a two-step resin film infusion process. In the first step, a prepreg is made from this prelaminated fabric. In the second step, several prepreg layers are stacked to form plates with an average thickness of 2.1 mm.

The lay-up that was used for the plates is $[-45,+45]_{2s}$. To ensure fully symmetrical plates, both a (+45,-45) fabric and a (-45,+45) fabric were used. In this way, the stitching directions in the different fabric layers in the plate are parallel to each other

The sample directions used for the mechanical tests are shown in figure 1. MD and CD stand for machine and cross direction respectively, BD+ is oriented so that the fibres in the outer layer of the sample lie parallel to the loading direction (i.e. the -45° direction), BD- is perpendicular to BD+ (i. e. the +45° direction). The average fibre volume fraction of the composite plates is 56%.

From the plates, samples with dimensions 250x25x2 mm³ were cut using a water cooled diamond saw. Composite end tabs were glued onto the samples, giving a gauge length of approximately 150 mm.

3 Static tensile tests

Static tensile tests were done in the four directions (BD+, BD-, MD and CD). The test speed was 1mm/min. Strain was measured with an extensometer. A minimum of five samples was tested in each direction. Acoustic emission sensors were attached to the samples, to determine the strain level ε_a at which damage starts to develop. This level is defined as the strain level at which the acoustic emission cumulative energy suddenly increases (figure 2).

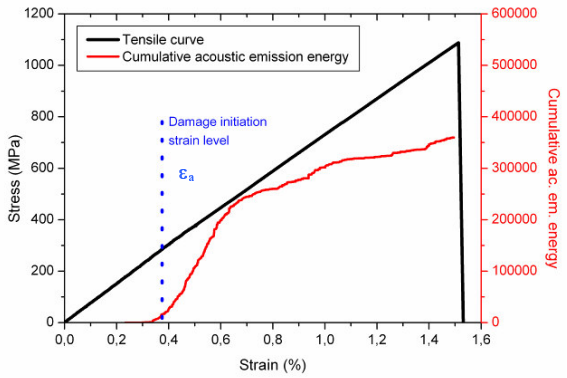

Fig. 2. Illustration of the determination of the ε_a strain level

Table 2: results for the static tensile tests in the different directions

	MD	CD	BD+	BD-
Stiffness (GPa)	15 ± 1	15 ± 2	68 ± 3	66 ± 1
Strength (MPa)	131 ± 1	121 ± 2	992 ± 25	1036 ± 41
Failure strain (%)	3.0 ± 0.2	2.4 ± 0.2	1.5 ± 0.1	1.6 ±0.1
ε_a strain level (%)	1.8 ± 0.1	1.6 ± 0.1	0.40 ± 0.05	0.36 ± 0.03
Stress at ε_a (MPa)	129	117	270	254
ε_{nl} strain level (%)	0.4	0.4	-	-
Stress at ε_{nl} (MPa)	50	50	-	-

The results for the static tests are given in table 2. It can be seen that the damage initiation strain level in the fibre directions BD+ and BD- is about 0.4%, and in the matrix dominated MD and CD directions it is about 1.6-1.8%.

Average tensile curves in MD and CD are given in figure 5. Samples tested in MD (parallel to the stitching) have a systematically higher strength and strain to failure than samples tested in CD. Assuming stitching sites can be seen as initiation places for damage, this can be explained by taking into account the difference in distance between the stitching sites in the two directions. This can be seen

in table 1 and figure 1, where the spacing between adjacent rows of stitching and the length of a stitch have been indicated. The stitch length (= the distance between subsequent sites on a line in MD) is smaller than the stitching spacing (= the distance between subsequent sites on a line in CD). So, if tension is applied in CD, more stitching sites or potential damage initiators are located on a line perpendicular to the tension direction, leading to earlier damage, lower strength and lower failure strain. The stiffness of the CD samples however, coincides with that of the MD samples, and the start of the non-linear behaviour occurs at the same strain level (ε_{nl}).

Samples tested in BD+ (and hence in the fibre direction) show a slightly lower strength than samples tested in BD-, while having a comparable stiffness and failure strain. This can also be seen from figure 3, which shows an example of a tensile curve in BD+ and BD-. The slope of the curve in BD+ can be seen to gradually decrease for strains higher than about 1%, while the curve in BD- remains linear up to failure. The decrease in modulus for the BD+ samples coincides with the appearance of strip-like 0° delaminations on the surface of the samples (figure 4). The reason for this behaviour is at present unclear, but the effect has been found by other researchers, e.g. Matsson et al.[11]. Their explanation starts from the assumption that the decrease in stiffness during the test, and hence the lower strength, is caused by failure and delamination of 0° bundles.

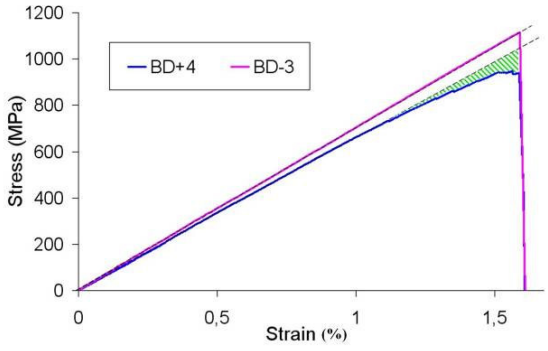

Fig. 3. Static tensile curve for a sample in BD- and BD+ , showing the decrease in modulus toward the end of the test in the latter (green hatched area).

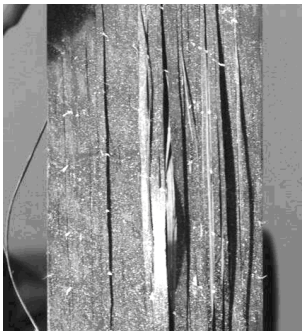

Fig. 4. Illustration of the striplike delaminations in the BD+ samples

However, it is also possible that there is an influence of the presence of the double transverse fibre layer in the middle of the BD+ samples (see figure 10). The double layer can be seen as one thick layer, and it has been shown in the past that thicker layers can have a negative influence on the properties [12, 13].

4 Fatigue tests

4.1 Fatigue tests up to $\varepsilon_a/\varepsilon_{nl}$

The stress levels corresponding to the damage initiation strain levels during the static tests were used as the maximum stress level for a series of tensile-tensile fatigue loading tests (R=0.1). As can be seen in figure 5, the stress level corresponding to the ε_a level in the MD and CD samples (fibres at ±45° to loading direction) is very close to the maximum stress level. As can be expected, the fatigue life of the samples at this stress level is very small (<5 cycles). Therefore, it was decided to use for the MD and CD samples the stress corresponding to the strain level ε_{nl} (approximately 0.4% strain, see table 2), at which the tensile curve starts to show a non-linear behaviour. This level is also indicated in figure 5. This means that the maximum fatigue stress level for all directions corresponds to a strain level of about 0.4% in a static test.

The fatigue tests were performed in load-controlled mode, at a frequency of 6 Hz and with a stress ratio of 0.1. Stress-strain data were collected during the tests using a dynamic extensometer. The maximum load levels for the fatigue tests are given in table 3.

It should be noted that, due to the much higher testing speed in the fatigue tests, compared to the static tests, the stiffness of samples in the matrix-dominated directions (MD and CD) will be significantly higher (about 5-10%) in the fatigue tests than in the static tests. This means that, even

though the tests are carried out to the stress level corresponding to the ε_a or ε_{nl} level, this strain level is never reached in the fatigue tests. In the fibre dominated directions (BD+ and BD-), this effect is negligible.

Samples were removed after a certain numbers of cycles ($5x10^5$, 10^6 and $5x10^6$ cycles). They were examined using X-ray radiography to monitor the development of damage during fatigue. The samples were immersed in a contrast medium (diiodomethane) for at least 12 hours prior to examination. The images were acquired using a Philips Tomohawk system and a 12 bit, 1024 x 1024 pixel resolution CCD camera.

Table 3: Fatigue load levels for the tests up to the ε_a or ε_{nl} stress levels

	BD+	BD-	MD/CD
ε_a (BD+ and BD-)/ε_{nl} (MD/CD)	0.4	0.36	0.4
Maximum fatigue load (MPa)	270	254	50

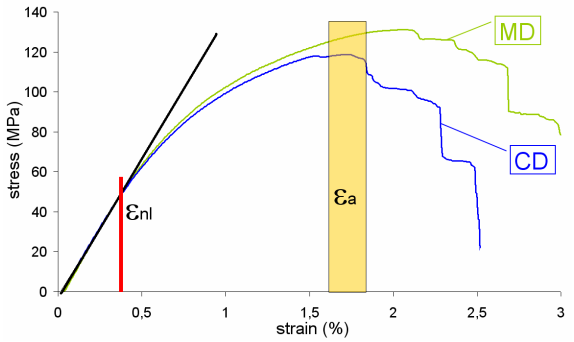

Fig. 5. Average stress-strain curves for MD and CD samples, indicating that the ε_a level for these directions is very close to the maximum stress level. The ε_{nl} level is defined as the strain level where the non-linearity of the curve begins

4.1.1 MD and CD results (matrix-dominated)

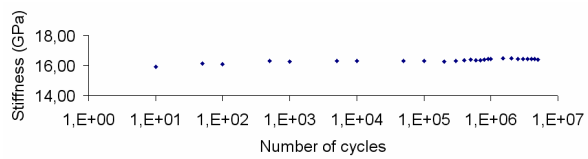

Fig. 6. Stiffness as a function of the number of fatigue cycles for an MD sample fatigue loaded up to the stress level corresponding to the start of the non-linear behaviour of the tensile curve

MD and CD samples did not fail up to $5x10^6$ cycles, and the stiffness of the samples did not decrease during the tests (figure 6).

Samples tested up to $5x10^5$, 10^6 and $5x10^6$ cycles were investigated with X-ray radiography, but no cracks or other damage were revealed. This means that the stress level of 50 MPa used for the fatigue tests can be considered a safe load level for this direction in this material.

4.1.2 BD+ and BD- results (fibre-dominated)

Samples fatigue tested in the fibre directions BD+ and BD- (σ_{max}=270/254 MPa) did not break up to $5x10^6$ cycles. No significant decrease in stiffness during the fatigue tests could be detected (figure 7). No macroscopic damage could be found on the samples. However, subsequent investigation of the samples with X-ray radiography revealed that there was a vast amount of transverse matrix cracks present in the tested samples. Figure 8 shows examples of X-ray images taken after different number of fatigue cycles.

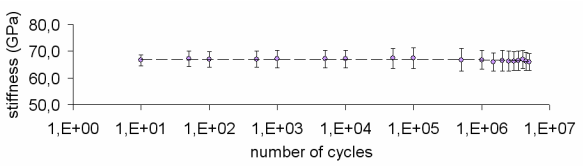

Fig. 7. Stiffness as a function of the number of fatigue cycles for BD+ samples fatigue loaded up to the stress level corresponding to the start of damage during a static test

The crack density was measured at $5x10^3$, $5x10^5$, 10^6 and $5x\ 10^6$ cycles in both BD directions to monitor the development of the damage. This was done as follows: on each X-ray image, 3 equally spaced vertical lines were drawn. For each of the lines, the number of intersecting cracks was determined. The average value for the 3 lines was then divided by the length of the lines. The results for the determination of the crack density can be found in figure 9.

It is remarkable to see that the crack density in BD+ is always higher (about 1.5 times) than in BD-. This contradicts what one might expect based on the number of transverse layers present in each type of sample (3 for BD+ and 4 for BD-, see figure 10).

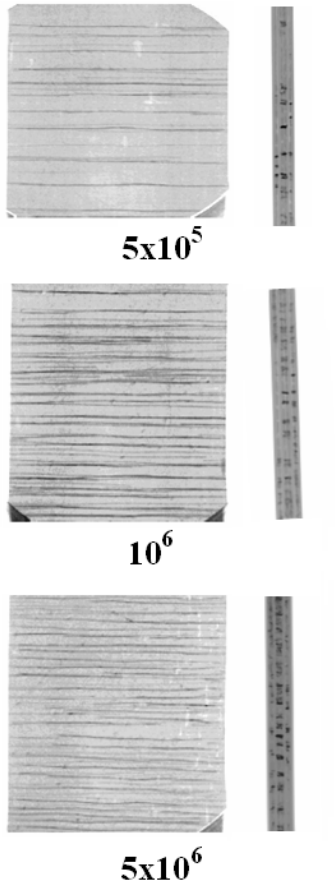

Fig. 8. X-ray images of BD+ samples tested in fatigue up to $5x10^5$, 10^6 and $5x10^6$ cycles. For each number of cycles, a front and a side view of a part of a sample are shown

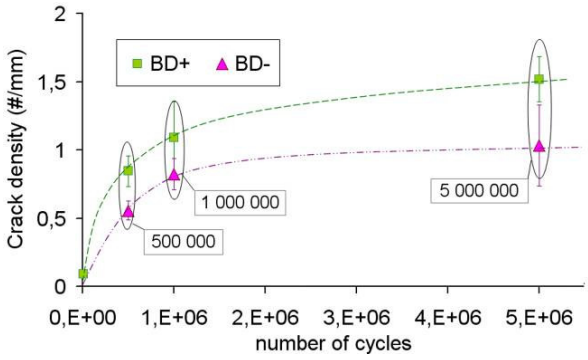

Fig. 9. Crack density as a function of the number of fatigue cycles in BD+ and BD- samples

However, it was seen during the X-ray investigation that there were almost no cracks in the two outer transverse layers of samples with BD- lay up. This might be explained by the influence of the free surface. Taking this into account, there are 3 effectively cracked inner layers in the BD+ samples and only 2 in the BD- samples, giving a ratio of 1.5, similar to the experimentally found ratio.

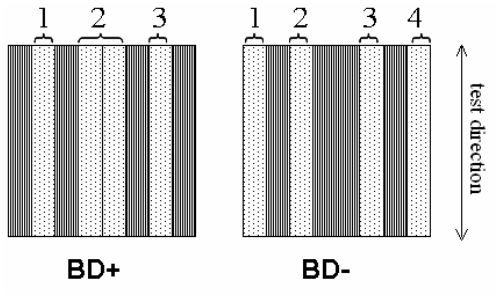

Fig. 10. Illustration of the number of transverse layers in BD+ and BD-

Like in the static tests, an influence of the lay-up on the behaviour of the material can thus be noticed here. In the static tests, it was concluded that the strength of BD+ oriented samples is somewhat lower than that of BD- oriented samples. Now it is found that also the crack density in BD+ samples after fatigue is higher than in BD- samples.

To determine the sensitivity of the material to the alignment of the fibre direction to the loading direction, a series of fatigue tests was done on 5° off-axis BD+ samples. This means that the fibre direction in the outer layer of the samples is 5° off-axis to the load direction. The load level used for these tests was the same as for the on-axis BD+ samples (max 270 MPa).

Table 4: Results for the fatigue life of samples tested in 5° off BD+ direction.

Sample	Fatigue life
1	521303
2	602414
3	599004
4	157000
5	351993
6	217486
7	122510
8	217399

Even though scatter on the results is large, it is evident that the fatigue life drops dramatically (from more than 5 million to less than a few hundreds of thousands of cycles, see table 4). This leads to the conclusion that it is very critical to make sure that fibres are aligned correctly during the manufacturing process. If, for some reason, the actual loading

condition in a real part would deviate 5° from that anticipated during production, this could have a detrimental effect on the performance of the part.

4.2 Post-fatigue tensile tests

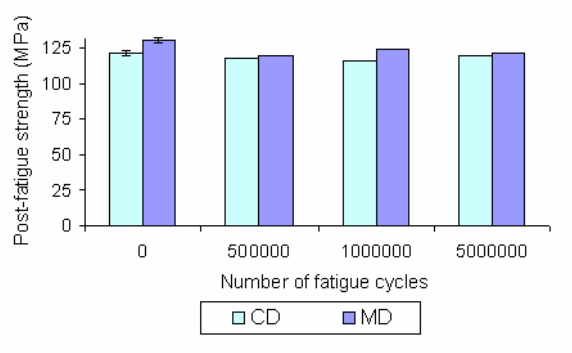

Fig. 11. Post fatigue tensile strength for samples tested in MD and CD. (only 1 sample per condition for N>0)

To investigate the influence of the fatigue loading on the static behaviour of the material, post-fatigue tensile tests were done on samples tested in fatigue for $5x10^5$, 10^6 and $5x10^6$ cycles. For the BD directions, these samples have been fatigue tested up to a stress corresponding to the damage initiation strain level (ε_a) during a static test, for the MD and CD directions samples have been tested up to the stress corresponding to the start of the non-linearity in the tensile curve.

The static tests were done at a speed of 1 mm/min. Three samples were tested per condition in BD+ and BD-, and one in MD and CD.

In MD and CD samples, no damage was found in the samples that were fatigue loaded up to the non-linearity stress level for $5x10^6$ cycles. It is therefore not surprising that the static properties of these samples are the same as for non-fatigue loaded samples. A chart of the post-fatigue tensile strength as a function of the number of fatigue cycles is shown in figure 11.

As was discussed in the previous paragraph, transverse cracking occurs in BD+ and BD- samples fatigue loaded up to the damage initiation stress level. The results for the tensile strength, the failure strain and the stiffness of these samples in the post-fatigue tests are shown in figure 12 and 13.

It can be seen from these graphs that even though the crack density increases with increasing number of fatigue cycles, as was stated above, the static properties are virtually unchanged. This is consistent with the absence of a significant reduction in dynamic stiffness during the fatigue tests, and is easily explained by the fact that properties in BD+ and BD- are for the major part determined by the fibres, which are not damaged during the fatigue cycling.

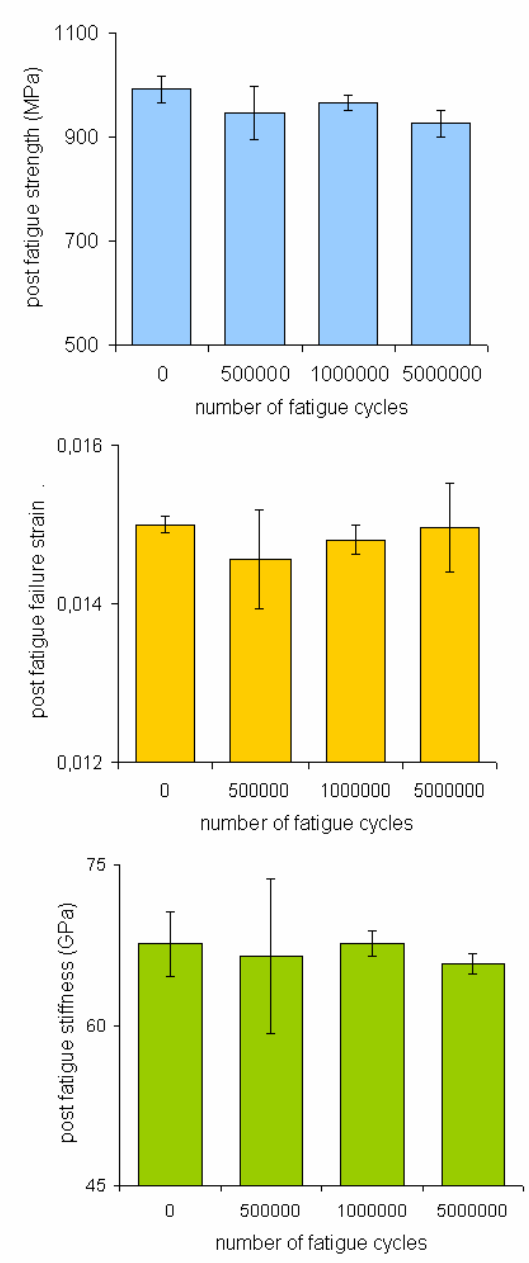

Fig. 12. Post-fatigue tensile properties for samples tested in BD+: strength (top), failure strain (middle) and stiffness (bottom)

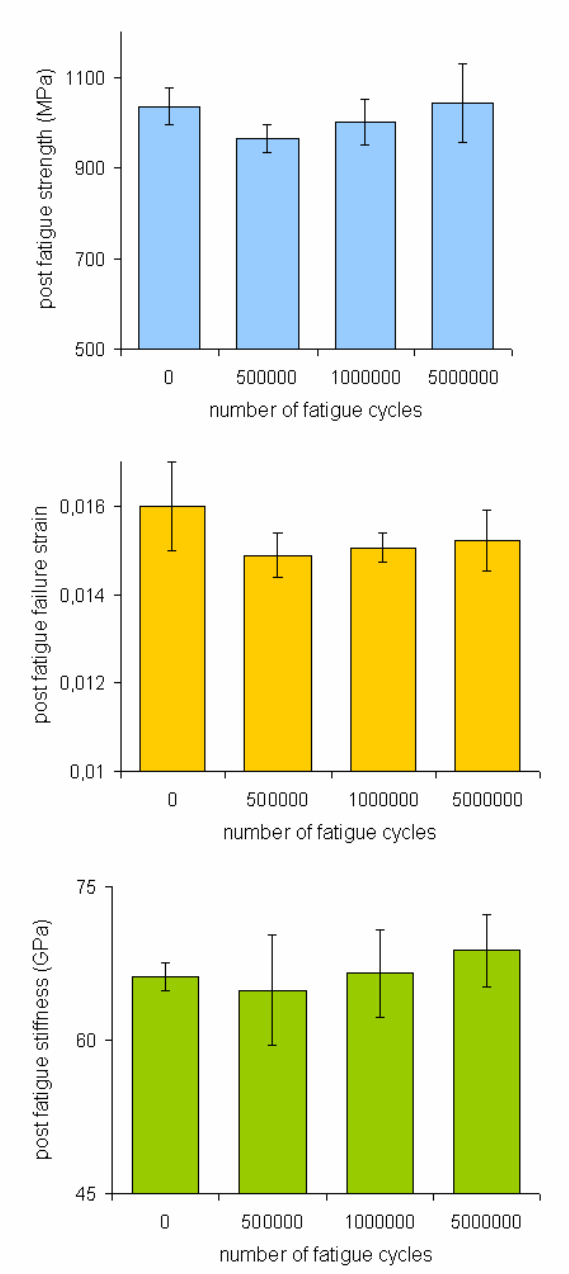

Fig. 13. Post-fatigue tensile properties for samples tested in BD+: strength (top), failure strain (middle) and stiffness (bottom)

4.3 Fatigue life distribution

Finally, a series of samples were fatigue loaded up to different load levels to determine the fatigue life at these loads. This allowed for a fatigue life curve to be made for each of the four directions. The results for MD and CD are shown in figure 14, those for BD+ and BD- in figure 15.

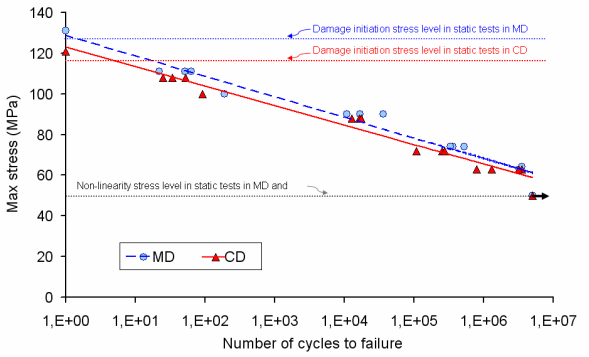

Fig. 14. Fatigue life curve for samples tested in the MD and CD directions

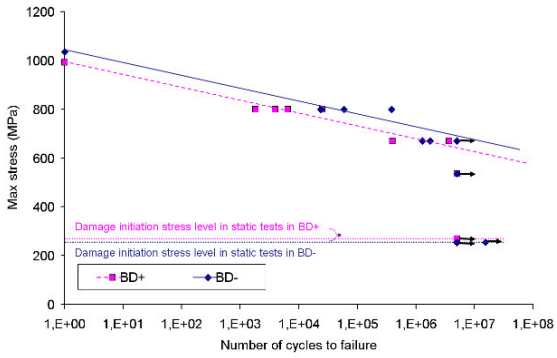

Fig. 15. Fatigue life curve for samples tested in the BD+ and BD- directions

The values for the damage initiation stress levels during a static test are also marked in the graphs, as well as the stress level where the MD and CD static tensile curves starts to behave non-linear (marked on the graph as 'non-linearity stress level').

It can be seen that MD and CD samples, fatigue loaded up to one half of the tensile strength, still have a fatigue life of about 10^6 cycles. In the fibre directions BD+ and BD-, the fatigue life at one half of the tensile strength is even higher (> 5 x 10^6).

This means that for most purposes, it can be assumed that the fatigue life of this material in the fibre directions is quasi-infinite (higher than 5 x 10^6) for stresses lower than one half of the tensile strength. It is remarkable to see that this stress level, which is about 500 MPa, is almost double the stress at damage initiation during a tensile test. It seems that the damage which is formed in samples, fatigue tested up to stresses about twice the damage initiation stress level, develops at such a slow rate that failure does not occur until very high cycle times, while in samples fatigue tested up to a higher

load level, the damage level increases more rapidly and the critical damage level for failure is reached at lower cycle times.

5 Conclusion

The fatigue and post-fatigue behaviour of carbon fibre – epoxy non crimp fabric composites was studied. Static tensile tests were done to determine the static properties and the stress-strain level at which damage starts to develop.

An influence of the lay-up, as well as of the stitching parameters on the static properties was noticed. The damage initiation stress level was used as the maximum stress level in tensile-tensile fatigue tests.

In the matrix dominated directions MD and CD, this leads to a very fast failure. Therefore, it was decided to test at a lower stress level, corresponding to the non-linearity stress level in a static test. These samples did not break up to $5x10^6$ cycles, showed no measurable dynamic stiffness decrease, and no damage could be found with x-ray radiography.Post-fatigue tests indicated no difference in behaviour between fatigue loaded and unloaded samples.

In fibre direction, transverse cracks were seen to develop during the fatigue tests at the damage initiation stress level. However, samples did not break up to $5x10^6$ cycles, and no significant decrease in dynamic stiffness was found. The post-fatigue tests did not reveal an influence of this fatigue damage on the strength, failure strain or stiffness of the samples. Fatigue life curves were determined for all four test directions.

References

[1] Edgren, F. and L.E. Asp. "Approximate analytical constitutive model for non-crimp fabric composites". *Composites Part A*, 2005. 36(2): p. 173-181.

[2] Edgren, F., L.E. Asp, and P.H. Bull. "Compressive Failure of Impacted NCF Composite Sandwich Panels – Characterisation of the Failure Process". *journal of composite materials*, 2004. 38(6): p. 495-514.

[3] Edgren, F., L.E. Asp, and R. Joffe. "Failure of NCF composites subjected to combined compression and shear loading". *Composites Science and Technology*, 2006. 66(15): p. 2865-2877.

[4] Edgren, F., et al. "Formation of damage and its effects on non-crimp fabric reinforced composites loaded in tension". *Composites Science and Technology*, 2004. 64(5): p. 675-692.

[5] Lomov, S.V., et al. "Carbon composites based on multiaxial multiply stitched preforms. Part 1. Geometry of the preform". *Composites Part A*, 2002. 33(9): p. 1171-1183.

[6] Loendersloot, R., et al. "Carbon composites based on multiaxial multiply stitched preforms. Part V: geometry of sheared biaxial fabrics". *Composites Part A*, 2006. 37(1): p. 103-113.

[7] Lomov, S.V., et al. "Carbon composites based on multiaxial multiply stitched preforms. Part 3: Biaxial tension, picture frame and compression tests of the preforms". *Composites Part A*, 2005. 36(9): p. 1188-1206.

[8] Lomov, S.V., et al. "Carbon composites based on multiaxial multiply stitched preforms. Part 2. KES-F characterisation of the deformability of the preforms at low loads". *Composites Part A*, 2003. 34(4): p. 359-370.

[9] Truong, T.C., et al. "Carbon composites based on multi-axial multi-ply stitched preforms. Part 4. Mechanical properties of composites and damage observation". *Composites Part A*, 2005. 36(9): p. 1207-1221.

[10] Vallons, K., et al. "Carbon composites based on multi-axial multi-ply stitched preforms. Part 6. Fatigue behaviour at low loads: stiffness degradation and damage development". *Composites Part A: Applied Science and Manufacturing*. In Press, Accepted Manuscript.

[11] Mattsson, D., R. Joffe, and J. Varna. "Damage in NCF composites under tension: effect of layer stacking sequence". *Engineering Fracture Mechanics*. In Press, Accepted Manuscript.

[12] Sihn, S., et al. "Experimental studies of thin-ply laminated composites". *Composites Science and Technology*. In Press, Corrected Proof.

[13] Tsai, S.W. "Thin ply composites". *JEC - composites*, 2005(18): p. 31-33.